An accurate two-stream moment method for kinetic boundary layer problems of linear kinetic equations

1992 J. Phys. A: Math. Gen. 25 1855

(http://iopscience.iop.org/0305-4470/25/7/026)

J. Phys. A: Math. Gen. 25 (1992) 1855-1874. Printed in the UK

An accurate two-stream moment method for kinetic boundary layer problems of linear kinetic equations

A J Kainz and U M Titulaer

Institut für Theoretische Physik, Johannes Kepler Universität Linz, A-4040 Linz, Austria

Received 4 October 1991

Abstract. We develop a method for solving 1D kinetic boundary layer problems for linear equations that uses separate Hermite moment expansions in the velocity variable for particles moving towards and away from a plane wall. This so-called two-stream method is tested for two especially simple kinetic equations, the linear BGK equation and the Klein-Kramers equation, the kinetic equation for Brownian particles. For both of these equations, extensive exact information is available for two simple boundary layer problems, the Milne and the albedo problem. A comparison of these exact results with those obtained with our version of the two-stream moment method shows that the accuracy obtainable by our method exceeds that of earlier methods by several orders of magnitude. In particular, the method allows us to obtain accurate results not only for the moments of the distribution function, but also for the distribution function itself. Small discrepancies remain close to the wall for small values of the velocity: the distribution function at the wall has a singularity at velocity zero, which can never be reproduced exactly by an approximation by piecewise analytic functions. For the albedo problem, in which particles are injected into the system at the wall with a given velocity distribution, we obtain reasonable results for the distribution of returning particles, even for input distributions for which the expansion in Hermite functions diverges or converges extremely poorly.

1. Introduction and survey

In the theory of kinetic boundary layers there are two classes of problems for which extensive exact analytic information is available. They involve the Klein-Kramers equation [1, 2] and the linear Bhatnagar-Gross-Krook (BGK) equation [3, 4] for a half-infinite space bounded by a plane wall that absorbs all or some of the particles that collide with it. The BGK case is solvable by quadratures [4, 5]; for the Klein-Kramers case a solution involving infinite series, with closed form expressions for several quantities of interest, was given a few years ago by Marshall and Watson [6]. The two problems are therefore well suited for testing approximate schemes for solving kinetic boundary layer problems.

Both the exact solutions and many approximate schemes involve a decomposition of the required solution in terms of special solutions: the Chapman-Enskog solutions, which vary slowly in space, and boundary layer eigensolutions, which decay in space on the scale of the mean free path (or the velocity persistence length in the Klein-Kramers case). In both cases these special solutions are known exactly. In the Klein-Kramers case the spectrum of decay lengths is discrete [7]; in the BGK case the spectrum is continuous and the associated eigenfunctions are distributions [8]. In the Klein-Kramers case, the expansion of the required solution in terms of the special solutions converges very slowly [9, 10], hence it is not well suited to obtain accurate numerical results. Better results, and in particular faster convergence, are obtained [11, 12] by

0305-4470/92/071855+20$04.50

first expanding the solution in terms of the Hermite polynomials in the velocity variable, truncating the resulting system of coupled ordinary differential equations, and expanding in terms of the special solutions of the truncated system. This method yields accurate results for moments of the distribution function, but the distribution function for the particles, especially at the wall, is still approximated rather poorly. This is not too surprising, since the functions used in the expansion are analytic ones, whereas the distribution function at the wall is known to be non-analytic, both in the Klein-Kramers [10, 13, 14] and in the BGK case [4, 15].

A treatment that gives accurate results already in low truncation orders was given by Gross *et al* [16] for the BGK and related models, and by Razi Naqvi *et al* [17], who generalized earlier work by Harris [18], for the Klein-Kramers case. In this approach, separate expansions are used for particles moving towards and away from the wall; hence the method is called the two-stream method. This ansatz naturally allows for non-analytic behaviour at the wall, though not precisely of the required type, at the price of also introducing singularities away from the wall, where the distribution function should be analytic [14, 15]. Thus it appears worthwhile to explore the behaviour of this approximation as the truncation order is increased. This is not easily done using the formalisms of [16] and [17]. The former uses a procedure that rapidly becomes numerically unsuitable as the truncation order is increased, whereas the second requires a fair amount of analytical labour for each order of truncation separately. Therefore, we developed a variant of the formalism of [16] in which the analytical preparations can be performed once and for all for an arbitrary truncation order. As a consequence, the order of truncation is limited merely by the accuracy obtainable in the numerical implementation of our algorithm.

In section 2 we present the kinetic equations treated in this paper, expand them in terms of half-range Hermite polynomials, and discuss some properties of this non-orthogonal system of basis functions. In section 3 we consider truncated versions of the system of coupled differential equations for the expansion coefficients, and the special solutions (Chapman-Enskog and boundary layer eigenfunctions) of this truncated set. We then give the procedure to be used to obtain the solutions for two especially simple stationary boundary layer problems, the stationary Milne problem (both for complete and for partial absorption at the wall) and the stationary albedo problem for injection of particles at the wall with a thermal distribution at a temperature different from that prevailing far from the wall.

The subsequent sections are devoted to a presentation of our results. In section 4 we present the results for the Milne problem with complete absorption. For both equations we obtain extremely accurate results for the moments, in particular for the so-called Milne extrapolation length, and very good results for the distribution function at the wall as well. Special attention is paid to the behaviour of the distribution function near the non-analytic point, and comparisons are made with known analytic results [14, 15]. Sections 5 and 6 are devoted to results for the Milne problem with partial specular reflection and the albedo problem, respectively. The final section contains a few concluding remarks, mainly on possible applications to more general problems.

2. Basic equations

The equations studied in this paper are of the form

$$v\frac{\partial}{\partial x}f(v,x)=\mathscr{C}f(v,x) \tag{2.1}$$

where $f(v, x)$ is the distribution function for the velocity v and the position x of the particle and $\mathscr{C}$ is a linear collision operator acting on v only; the left-hand side describes the free flow of the particles. The form (2.1) is purely 1D; its relevance for 3D problems in a half-space bounded by a plane wall will be discussed briefly in section 7. Moreover, (2.1) as written applies only to stationary situations. Although the Laplace transform of the corresponding time-dependent equation also takes the form (2.1), with a slightly modified $\mathscr{C}$ [4, 9], the inversion of the Laplace transform and the treatment of the initial conditions involve additional problems that exceed the scope of the present paper.

We study two examples for $\mathscr{C}$: the Klein-Kramers operator $\mathscr{C}_K$ and the BGK-operator $\mathscr{C}_B$, which in suitable dimensionless units take the form

$$\mathscr{C}_K = \frac{\partial}{\partial v}\left(v + \frac{\partial}{\partial v}\right) \tag{2.2a}$$

$$\mathscr{C}_B = 1 - \phi_0(v) \int \mathrm{d}v' \tag{2.2b}$$

where $\phi_0(v) = (2\pi)^{-1/2} \exp[-v^2/2]$ is the Maxwell equilibrium distribution in scaled units. The operators $\mathscr{C}_i$ are self-adjoint with respect to the scalar product

$$\langle f, g\rangle \equiv \int \mathrm{d}v f^*(v) g(v) \phi_0(v)^{-1}. \tag{2.3}$$

The eigenfunctions of both $\mathscr{C}_K$ and $\mathscr{C}_B$ may be chosen as

$$\phi_n(v) = \phi_0(v)\psi_n(v) \tag{2.4a}$$

$$\psi_n(v) = \frac{1}{\sqrt{2^n n!}} H_n\left(\frac{v}{\sqrt{2}}\right) \tag{2.4b}$$

where $H_n(y)$ is the nth Hermite polynomial. (Note that our normalization of the $\phi_n(v)$ differs from that used in earlier work [12, 19].) The corresponding eigenvalues are

$$\varepsilon_{Kn} = -n \qquad \varepsilon_{Bn} = \delta_{n0} - 1. \tag{2.5}$$

The eigenfunctions are connected by the ladder operators

$$a^+ = -\partial/\partial v \qquad a^- = v + \partial/\partial v \tag{2.6}$$

which satisfy the relations

$$a^+ \phi_n = \sqrt{n+1}\, \phi_{n+1} \qquad a^- \phi_n = \sqrt{n}\, \phi_{n-1}. \tag{2.7}$$

We shall expand the solution to be constructed in terms of the half-range functions:

$$f(v, x) = \sum_{n=0}^{\infty} [B_n^+(x)\phi_{n+}(v) + B_n^-(x)\phi_{n-}(v)] \tag{2.8}$$

with

$$\phi_{n\sigma}(v) = \phi_n(v)\Theta(\sigma v) \qquad \sigma = \pm 1. \tag{2.9}$$

The system of functions $\phi_{n\sigma}$ is not orthonormal; we have instead

$$\langle \phi_{n\sigma}, \phi_{m\tau}\rangle \equiv a_{nm}^{\sigma\tau} = \delta_{\sigma\tau} a_{nm} \tag{2.10a}$$

with a_{nm} given by

$$a_{nm} = \delta_{nm}/2 \qquad \text{for } n+m \text{ even} \tag{2.10b}$$

$$a_{2n,2m+1} = \frac{(-1)^{n+m}(2n-1)!!}{(2m)!!(2m-2n+1)} \sqrt{\frac{(2m+1)!}{2\pi(2n)!}} \tag{2.10c}$$

$$a_{2m+1,2n} = a_{2n,2m+1}. \tag{2.10d}$$

The particle and current density contained in (2.8) are given by

$$n(x) \equiv \int \mathrm{d}v f(v,x) = \sum_n a_{0n}[B_n^+(x) + (-1)^n B_n^-(x)] \tag{2.11a}$$

$$j(x) \equiv \int \mathrm{d}v\, v f(v,x) = \sum_n a_{1n}[B_n^+(x) - (-1)^n B_n^-(x)]. \tag{2.11b}$$

Taking matrix elements of (2.1) with respect to the set of functions (2.9) we obtain the set of equations

$$\frac{\partial}{\partial x} \sum_{m\tau} \mathbb{S}_{nm}^{\sigma\tau} B_m^\tau(x) = \sum_{m\tau} \mathbb{C}_{nm}^{\sigma\tau} B_m^\tau(x) \tag{2.12}$$

with $\mathbb{S}$ a symmetric matrix with elements

$$\mathbb{S}_{nm}^{\sigma\tau} = \langle \phi_{n\sigma} | v | \phi_{m\tau} \rangle = \sqrt{m+1}\, a_{n,m+1}^{\sigma\tau} + \sqrt{m}\, a_{n,m-1}^{\sigma\tau} \tag{2.13}$$

that are easily calculated using (2.7) and (2.10a). The matrix ${}^{\mathrm{B}}\mathbb{C}$ corresponding to $\mathscr{C}_{\mathrm{B}}$ is also readily found from (2.2b):

$${}^{\mathrm{B}}\mathbb{C}_{nm}^{\sigma\tau} = -a_{nm}^{\sigma\tau} + a_{n0}^{\sigma\sigma} a_{0m}^{\tau\tau}. \tag{2.14}$$

The evaluation of the matrix ${}^{\mathrm{K}}\mathbb{C}$ corresponding to $\mathscr{C}_{\mathrm{K}}$ requires special care due to the action of the differentiations on the Θ-functions:

$$\mathscr{C}_{\mathrm{K}} \phi_{n\sigma}(v) = (-n)\phi_{n\sigma}(v) + 2\sigma\delta(v)\phi_n'(v) + \sigma\phi_n(v)\delta'(v). \tag{2.15}$$

To evaluate integrals involving this distribution we use the rules

$$\int_0^\infty \mathrm{d}v\, \delta(v) g(v) = \tfrac{1}{2} g(0) \tag{2.16a}$$

$$\int_0^\infty \mathrm{d}v\, \delta'(v) g(v) = -\tfrac{1}{2} g'(0) - g(0)\delta(0) \tag{2.16b}$$

which can be obtained by formal integration by parts or by substitution of a representation of the δ-function. The corresponding expressions for integrals from $-\infty$ to 0 are found by a transformation of variables. Using these rules, (2.7), and the known properties of the Hermite polynomials, we obtain

$${}^{\mathrm{K}}\mathbb{C}_{nm}^{\sigma\tau} = -m a_{nm}^{\sigma\tau} + \frac{\tau}{2}(m-n) a_{nm} - \sigma\tau\sqrt{2\pi}\, \phi_n(0)\phi_m(0)\delta(0). \tag{2.17}$$

Both (2.14) and (2.17) are symmetric matrices; for (2.17) this can be seen using (2.10). Moreover they obey the relation

$$\sum_\sigma \mathbb{C}_{0m}^{\sigma\tau} = 0 \qquad \text{for all } m \text{ and } \tau \tag{2.18}$$

which expresses conservation of current [ϕ_0 is a left eigenfunction of $\mathscr{C}$ with eigenvalue zero with respect to the scalar product (2.3)].

The occurrence of $\delta(0)$ contributions looks disturbing at first sight. Such contributions can be avoided if one uses a mixed representation

$$\mathbb{S}^{\cdot\sigma}_{mn} = \langle \phi_m | v | \phi_{n\sigma} \rangle \qquad \mathbb{C}^{\cdot\sigma}_{mn} = \langle \phi_m | \mathscr{C} | \phi_{n\sigma} \rangle. \tag{2.19}$$

In this representation all matrix elements are regular. In fact, the results shown in some of the figures of [14] were obtained using such a mixed representation. Meanwhile, we found that the formalism just presented not only yields symmetrical matrices, but gives much more accurate numerical results as well. We therefore shall not present the formalism based on (2.19) in any more detail, but occasionally mention the results obtained by it for purposes of comparison.

In the formalism of [16], the expansion (2.8) is replaced by an expansion in terms of an orthogonal set of functions, obtained from the $v^n \phi_{0\sigma}$ (or from the $\phi_{n\sigma}$) by means of the Gram–Schmidt orthonormalization procedure. This has the advantage of leading to simpler expressions for $\mathbb{S}$ and ${}^{B}\mathbb{C}$; the algorithm for the recursive calculation of the orthogonal functions quickly becomes numerically intractable, however. This also means that the construction of ${}^{K}\mathbb{C}$, and of other collision operators with explicitly known eigenfunctions, may become awkward. Since our formalism and that of [16] are in principle equivalent, the choice between them becomes one of numerical (and algebraic) convenience; in view of the excellent convergence properties of our method, we did not carry out extensive calculations using the formalism of [16].

3. Special solutions and boundary layer problems

In this section we consider the truncated version of (2.12), obtained by restricting the indices n and m to $0 \leqslant n, m \leqslant N-1$†. The truncated version of $\mathbb{C}$, like (2.2), is negative semidefinite with a single eigenfunction belonging to $\lambda = 0$. The truncated version of $\mathbb{S}$ has only non-zero semisimple eigenvalues, in pairs of opposite sign. We shall use the same notation as in (2.12) for the truncated quantities as long as there is no danger of confusion; if we wish to consider the dependence on N, an upper index (N) will be added to the quantity under consideration. We are interested in particular in solutions of the form

$$B^{\sigma}_{n}(x) = \exp[-\lambda_k x] b^{\sigma}_{n(k)}. \tag{3.1}$$

The $\boldsymbol{b}_{(k)}$, i.e. the vectors with components $b^{\sigma}_{n(k)}$, obey the generalized eigenvalue equation

$$-\lambda_k \mathbb{S} \cdot \boldsymbol{b}_{(k)} = \mathbb{C} \cdot \boldsymbol{b}_{(k)} \tag{3.2}$$

or, since $\mathbb{S}$ is invertible, at least in its truncated form‡,

$$\mathbb{S}^{-1} \cdot \mathbb{C} \cdot \boldsymbol{b}_{(k)} = -\lambda_k \boldsymbol{b}_{(k)}. \tag{3.3}$$

With the exception of $\lambda_0 = 0$, all eigenvalues of (3.3) are semisimple and they occur in pairs of opposite sign. For $\lambda = 0$ we have the Jordan case: the two vectors

$$b^{\sigma}_{n(0)} = \delta_{n0} \qquad b^{\sigma}_{n(1)} = -\delta_{n1} \tag{3.4}$$

† In a formalism based on (2.19) the corresponding restriction would be $0 \leqslant m \leqslant 2N-1$; $0 \leqslant n \leqslant N-1$.

‡ Though $\mathbb{S}$ is invertible for any finite N, half of its eigenvalues approach zero with increasing N, due to the overcompleteness of the $\phi_{n\sigma}$. The same holds for $\mathbb{C}$, but the combination $\mathbb{S}^{-1} \cdot \mathbb{C}$ stays well behaved with increasing N. The mentioned property of $\mathbb{S}$ restricts us to values of N smaller than 30; then, the lowest eigenvalues become indistinguishable from zero numerically, even in extended precision calculations.

obey the relations

$$\mathbb{C} \cdot \boldsymbol{b}_{(0)} = 0 \qquad \mathbb{C} \cdot \boldsymbol{b}_{(1)} = \mathbb{S} \cdot \boldsymbol{b}_{(0)}. \tag{3.5}$$

We shall arrange the other $\boldsymbol{b}_{(k)}$ in ascending order of the $|\lambda_{(k)}|$, in such a way that the $\boldsymbol{b}_{(2l)}$ and $\boldsymbol{b}_{(2l+1)}$ belong to positive and negative λ, respectively. From the symmetry of $\mathbb{C}$ the relation

$$(\lambda_k - \lambda_l)\boldsymbol{b}_{(k)} \cdot \mathbb{S} \cdot \boldsymbol{b}_{(l)} = 0 \qquad (k, l \neq 0, 1) \tag{3.6}$$

follows. Hence, we may normalize the $\boldsymbol{b}_{(l)}$ according to

$$\boldsymbol{b}_{(k)} \cdot \mathbb{S} \cdot \boldsymbol{b}_{(l)} = \delta_{kl} \operatorname{sgn}(\lambda_k). \tag{3.7a}$$

The quantity on the left in (3.7a) also vanishes when k or l, but not both, take the value 0 or 1. The remaining values are

$$\begin{aligned} &\boldsymbol{b}_{(0)} \cdot \mathbb{S} \cdot \boldsymbol{b}_{(0)} = \boldsymbol{b}_{(1)} \cdot \mathbb{S} \cdot \boldsymbol{b}_{(1)} = 0 \\ &\boldsymbol{b}_{(0)} \cdot \mathbb{S} \cdot \boldsymbol{b}_{(1)} = \boldsymbol{b}_{(1)} \cdot \mathbb{S} \cdot \boldsymbol{b}_{(0)} = -1. \end{aligned} \tag{3.7b}$$

For the Klein-Kramers case the problem (3.3) just sketched cannot yet be solved, due to the occurrence of the $\delta(0)$. These delta-functions result from the action of the operator $\partial^2/\partial v^2$ on the Θ functions in the $\phi_{n\sigma}(v)$. They may thus be eliminated by a regularization of this operator. If we replace the Fourier transform $-q^2$ of $\partial^2/\partial v^2$ by $-\min(q^2, q_{\max}^2)$, the $\delta(0)$ is replaced by $\pi^{-1}q_{\max}$ (apart from some additional modifications that vanish for $q_{\max} \to \infty$). We therefore decided to replace $\delta(0)$ by a sufficiently large positive number†. This number should in any case be larger than the largest wavenumber in the Fourier transform of $f(u, x)$ with respect to u that we may expect to be reproduced faithfully in our approximation; hence the lower bound on '$\delta(0)$' should increase with N, as we also found heuristically. In practice, 10^3 turns out to be sufficiently large for all values of N considered. For still larger choices, most results do not change appreciably any more (though very large choices cause numerical difficulties in the calculation of eigenvalues and eigenvectors); see, however, the remarks at the end of section 5. As a test we considered the eigenvalues $\lambda_k^{(N)}$, which for large N must approach the exact eigenvalues [7]:

$$\lim_{N\to\infty} \lambda_{2k}^{(N)} = \sqrt{k} \qquad \lim_{N\to\infty} \lambda_{2k+1}^{(N)} = -\sqrt{k}. \tag{3.8}$$

The corresponding eigenfunctions

$$\ell_k^{(N)}(v) = \sum_{n=0}^{N-1} (b_{n(k)}^{+(N)} \phi_{n+}(v) + b_{n(k)}^{-(N)} \phi_{n-}(v)) \tag{3.9}$$

must approach the known Pagani eigenfunctions [7] for $N \to \infty$, in particular, they must become continuous at $v = 0$; for the jump $\Delta_k^{(N)}$ at $v = 0$ we thus require

$$\lim_{N\to\infty} \Delta_k^{(N)} \equiv \lim_{N\to\infty} \left[\sum_{m=0}^{(N-1)/2} (b_{2m(k)}^{+(N)} - b_{2m(k)}^{-(N)}) \phi_{2m}(0) \right] = 0. \tag{3.10}$$

In table 1 we present some $\lambda_{(k)}^{(N)2}$ and $\Delta_k^{(N)}$ for $N = 25$ and '$\delta(0)$' equal to 10^3 and 10^6. For low k, the limits (3.8) and (3.10) are already approached quite closely, independent

† As an alternative regularization method we modified $\mathscr{C}_K$ by replacing all eigenvalues of magnitude larger than M by $-M$, for some $M \gg N$. This required more computational effort, but led to similar, though slightly inferior, numerical results.

Table 1. The square of the decay length λ_{2n}^2 for some of the approximate boundary layer eigenfunctions obtained from the set of coupled moment equations for the Klein–Kramers case, truncated at $N=25$, using (hyb) the hybrid formalism based on (2.19), (2, *E*3) the consistent two-stream method with '$\delta(0)$' $=10^3$ and (2, *E*6) the same method with '$\delta(0)$' $=10^6$. The last column gives the jump Δ_{2n} in the velocity distribution at $v=0$, calculated with '$\delta(0)$' $=10^3$. The corresponding values for '$\delta(0)$' $=10^6$ (not shown) are somewhat smaller, but of the same orders of magnitude.

n	(hyb)	(2, *E*3)	(2, *E*6)	Δ_{2n}
1	$1+2\times10^{-31}$	$1+2\times10^{-30}$	$1+4\times10^{-28}$	-0.469×10^{-18}
2	$2-2\times10^{-26}$	$2+1\times10^{-20}$	$2+1\times10^{-20}$	0.424×10^{-13}
3	$3+5\times10^{-23}$	$3+2\times10^{-14}$	$3+2\times10^{-14}$	0.458×10^{-10}
5	$5+7\times10^{-14}$	$5+9\times10^{-7}$	$5+9\times10^{-7}$	0.238×10^{-6}
10	10.0614	12.1714	12.1717	-0.132×10^{-3}
15	0.2466×10^{2}	0.8165×10^{2}	0.8167×10^{2}	0.541×10^{-3}
20	0.2117×10^{3}	0.9195×10^{4}	0.9205×10^{4}	-0.473×10^{-2}
22	0.1501×10^{4}	0.7231×10^{6}	0.7259×10^{6}	-0.265×10^{-1}
23	0.9424×10^{4}	0.3711×10^{8}	0.3756×10^{8}	0.124×10^{0}
24	0.5603×10^{6}	0.9342×10^{12}	0.9576×10^{15}	0.141×10^{2}

of the choice of '$\delta(0)$'. For the BGK case, the spectrum of the operator in (3.3) should become continuous (apart from the discrete eigenvalue zero), hence there is no special significance to be attached to limits of the $\lambda_k^{(N)}$ and $\Delta_k^{(N)}$. Nevertheless, here also the $\Delta_k^{(N)}$ become small for $k \ll N$.

A solution of (2.1) in the half-space $x>0$ that increases no faster than linearly with increasing x can be approximated by

$$f^{(N)}(v,x)=d_0^{(N)}\phi_0(v)+d_1^{(N)}[\phi_1(v)-x\phi_0(v)] + \sum_{k=1}^{N-1} d_{2k}^{(N)} \exp[-\lambda_{2k}^{(N)}x] \sum_{n=0}^{N-1} [b_{n(2k)}^{+(N)}\phi_{n+}(v)+b_{n(2k)}^{-(N)}\phi_{n-}(v)]. \tag{3.11}$$

The form of the term containing $d_1^{(N)}$ follows from (3.4) and (3.5) and is familiar from earlier work [9, 10]. In the limit $N\to\infty$ the solution (3.11) is determined uniquely [6, 20] by the specification of either d_0 or d_1 and the additional requirement

$$f(v,0)=g(v) \qquad \text{for } v>0 \tag{3.12}$$

with a given function $g(v)$. Two well known solutions are the Milne solution f^{M}:

$$d_1^{\mathrm{M}}=-1 \qquad g(v)=0 \tag{3.13}$$

and the albedo solution for a particular function $g_{\mathrm{A}}(v)$

$$d_1^{\mathrm{A}}=0 \qquad g(v)=g_{\mathrm{A}}(v). \tag{3.14}$$

The condition (3.12) can be satisfied approximately by requiring that the expression

$$f_+^{(N)}(v,0)=d_0^{(N)}\phi_{0+}(v)+d_1^{(N)}\phi_{1+}(v)+\sum_{k=1}^{N-1} d_{2k}^{(N)} \sum_{n=0}^{N-1} b_{n(2k)}^{+(N)}\phi_{n+}(v) \tag{3.15}$$

has the same first N half-range moments as $g(v)$:

$$\int \mathrm{d}v f_+^{(N)}(v,0)\psi_{n+}(v)=\int \mathrm{d}v\, g(v)\psi_{n+}(v)\equiv g_n \qquad \text{for } 0\leqslant n<N \tag{3.16}$$

with the ψ_{n+} defined in analogy with (2.4*a*) and (2.9). These conditions suffice to determine the N coefficients $d_{2k}^{(N)}$ for $0\leqslant k<N$. In view of the overcompleteness of

the ψ_{n+} in the limit $N \to \infty$, the prescription (3.16) is not the only one which yields a sequence of $f^{(N)}$ that fulfils (3.12) for $N \to \infty$. However, it appears to be the natural analogue of the Marshak prescriptions [21] for full-range expansions, which for the same reason is also not unique. Moreover, as we shall see in the subsequent sections, the recipe (3.16) is practicable and it yields accurate numerical results.

4. The Milne problem for an absorbing wall

In the classical Milne problem, defined by (3.13), a constant particle current of unit strength flows towards an absorbing wall at $x = 0$. Such a situation may occur when the wall binds the particles chemically or when it is composed of a solid (or covered by a liquid layer) in contact with its supersaturated vapour. The solution of type (3.11) is obtained by putting $d_1^{(N)} = -1$ for all N and requiring the coefficient of each $\phi_{n+}(v)$ in (3.15) to vanish separately. This programme was carried out for $N \leq 30$, for the BGK and Klein-Kramers collision operators, with '$\delta(0)' = 10^3$ for the latter case. In figure 1 we show the resulting distribution $f_M^{(25)}(v, 0)$ at the wall for the BGK case. Also shown is the result of an expansion in full-range Hermite polynomials [11] with $N = 50$ (same number of parameters) and the result of the exact solution [4, 15]. An asymptotic evaluation of the BGK result around $v = 0$ yields [15]

$$f_{MB}(-v, 0) = \frac{1}{\sqrt{2\pi}} - \frac{v \ln v}{2\pi} + \frac{0.724\,71\ldots}{\sqrt{2\pi}}\, v + \mathcal{O}(v^2 \ln^2 v). \tag{4.1}$$

We see that the jump in f_{MB} at $v = 0$ is reproduced extremely well; the very weak singularity of type $v \ln v$ can of course not be reproduced completely by a piecewise analytic approximation, but the discrepancy is not visible in the figure. The magnitude of the discrepancy at $v = 0$ can be seen from the tables presented later in this section. For the Klein-Kramers case results similar to those presented were already given in figure 2 of [14], though with two-stream results obtained by the formalism based on (2.19). The version of the two-stream method given in this paper yields even better agreement with the exact asymptotic expressions for small v; for further details we refer to the tables to be discussed presently.

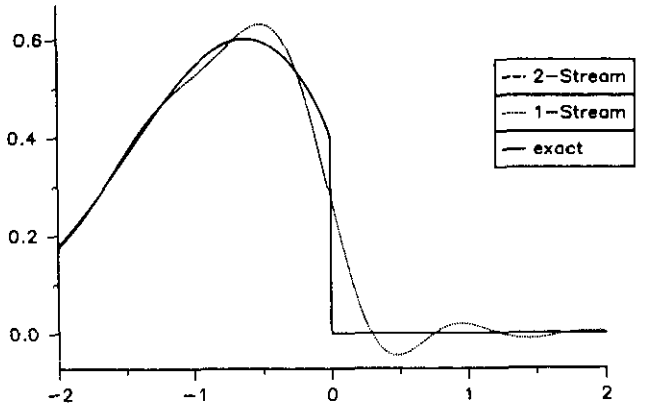

Figure 1. The Milne solution $f^M(v, 0)$ at the wall for the BGK case as obtained from the one-stream moment method with $N = 50$ and from the two-stream method with $N = 25$. The exact expression is indistinguishable from the latter result.

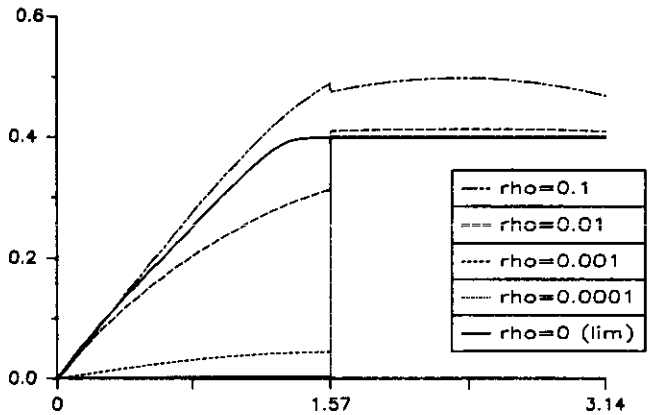

Figure 2. The Milne solution $f^{M}(\rho \cos \gamma, \rho \sin \gamma)$ for the BGK case, in $N = 28$ approximation, around the singularity $v = x = 0$ as a function of the angle γ for various small ρ. The exact $\rho \downarrow 0$ limit is indicated for comparison.

For several quantities characterizing the solution, accurate estimates can be obtained by evaluating the results for a number of truncation orders N and fitting the results $q^{(N)}$ to the formula

$$q^{(N)} = q_\infty + \gamma N^{-\delta}. \tag{4.2}$$

If a trend remains in the q_∞ obtained by fitting different groups of $q^{(N)}$, the procedure is repeated; this is roughly equivalent to adding more terms in (4.2). The existence of a formula of type (4.2) as an asymptotic expansion can be proved [10, 14] for approximations by finite series of exact boundary layer eigenfunctions; in the present context it should be considered a purely heuristic assumption. This procedure was carried out for the Milne extrapolation length

$$x_M \equiv d_0^M. \tag{4.3}$$

x_M is also the coordinate at which the extrapolated asymptotic density profile

$$n_{as}^{M}(x) = \int dv f_{as}^{M}(v, x) = x + x_M \tag{4.4}$$

where f_{as}^{M} is the distribution function without its boundary layer components, becomes zero. For the Klein-Kramers case the value found for $x_M^{(25)}$ did not change by more than 10^{-6} when the value for '$\delta(0)$' was varied between 50 and 10^8, in spite of the somewhat larger discrepancies seen for some quantities in table 1. Hence we shall restrict ourselves from now on to values calculated with '$\delta(0)$' = 10^3. We also estimated the particle density at the wall

$$n^{M}(0) = \int dv f^{M}(v, 0) \tag{4.5}$$

and the jump in the distribution function at $v = x = 0$

$$\Delta^{M} = \lim_{\varepsilon \downarrow 0} f^{M}(-\varepsilon, 0). \tag{4.6}$$

In tables 2 and 3 we give the results obtained for these quantities, both for $N = 30$ and by the (repeated) extrapolation procedure (4.2), for the BGK and Klein-Kramers

Table 2. The Milne length x_M, the density at the wall $n_M(0)$ and the velocity jump Δ^M for the Milne solution in the BGK case as calculated: (1s) by the one-stream method [12]; (2h) from the hybrid two-stream method based on (2.19); (2N) from the two-stream method in $N=30$ approximation; (2s) from the two-stream method with the repeated fit (4.2), which was also used to obtain the results (1s) and (2h), and (ex) by numerical integration of the exact analytic solution [15]. The quantity $n^M(0)$ in the (2N) approximation is found to be equal to unity up to the numerical round-off errors associated with the inversion of the matrix $\mathbb{S}$; this error increases from 3×10^{-31} for $N=2$ to 4×10^{-10} for $N=30$. A dash indicates that no fit was possible. Unless specified otherwise, the errors in fitted quantities are at most one unit in the last specified digit.

	x_M	$n^M(0)$	Δ^M
1s	1.437 1	1.000	—
2h	1.437 111	0.9999	0.427
2N	1.437 111 675 8...	1	0.400 7...
2s	1.437 111 685 7	1	0.398 94
ex	1.437 111 685 76...	1	0.398 942 28...

Table 3. The same quantities as given in table 2 for the Klein-Kramers case. The additional row (BT) gives the result of approximations by finite linear combinations of exact eigenfunctions [9, 10]; the entries in the row (ex) are obtained in closed form from the exact solution, except $n_M(0)$, which was obtained from a slowly converging exact series expression [14].

	x_M	$n^M(0)$	Δ^M
1s	1.460 35	0.936	—
2h	1.460 354 6	0.936 1	0.008
2N	1.460 354 85...	0.935 88...	0.0172...
2s	1.460 354 50	0.936 11	—
ex	1.460 354 508 809...	0.936 1145...	0
BT	1.461	0.95 ∓ 0.02	0.2 ∓ 0.3

cases, respectively. For comparison we also give the results obtained from the exact solutions [14, 15], from the formalism based on (2.19), from an expansion in full-range Hermite polynomials [11] and, in the Klein-Kramers case, from an approximation by finite linear combinations of exact boundary layer eigenfunctions [9, 10]. The exact value for x_M in the BGK case in our units is

$$x_M^{BGK}=\int_0^\infty \mathrm{d}t\,\frac{t\phi_0(t)}{\{\pi^2t^2\phi_0(t)^2+[1-\sqrt{2}\,tF_D(t/\sqrt{2})]^2\}} \tag{4.7a}$$

where F_D is Dawson's integral

$$F_D(x)=\exp[-x^2]\int_0^x \mathrm{d}t\,\exp[t^2]. \tag{4.7b}$$

The entry in table 2 was obtained by a new, accurate evaluation of the integrals in (4.7), since the literature values were too imprecise for assessing the accuracy of our formalism. In all comparative cases, only the extrapolated results are given. The results clearly show the improvement in numerical accuracy obtained, especially in the Klein-Kramers case, as we move ever further away from the exact eigenfunctions.

The BGK solution shows a particularly interesting singularity structure in the (v, x)-plane. As we approach the origin in this plane the limit obtained by asymptotic analysis of the exact solution [15] is

$$f_{\mathrm{B}}^{\mathrm{M}}(v, \alpha v) \simeq \frac{1}{\sqrt{2\pi}}(1-\mathrm{e}^{-\alpha}) + \mathcal{O}(v \ln v) \qquad v, \alpha \geqslant 0 \tag{4.8a}$$

$$f_{\mathrm{B}}^{\mathrm{M}}(-v, \alpha v) \simeq \frac{1}{\sqrt{2\pi}} + \mathcal{O}(v \ln v) \qquad v, \alpha \geqslant 0. \tag{4.8b}$$

In figure 2 we show how this limit is approached by plotting $f_{\mathrm{B}}^{\mathrm{M}}(\rho \cos \phi, \rho \sin \phi)$ as a function of ϕ for various ρ together with the limit (4.8) for $\rho \downarrow 0$. We see that serious discrepancies occur only for $\rho \leqslant 0.1$.

The method presented in this paper has one principal drawback: the approximations to the functions $f^{\mathrm{M}}(v, x)$ are non-analytic not only at $v = x = 0$, where an actual non-analyticity occurs, but also everywhere along the line $v = 0$. To assess the severity of this shortcoming we calculated the jump

$$\Delta_{\mathrm{M}}^{(28)}(x) \equiv \lim_{\varepsilon \downarrow 0} [f_{\mathrm{M}}^{(28)}(-\varepsilon, x) - f_{\mathrm{M}}^{(28)}(\varepsilon, x)] \tag{4.9}$$

for the BGK case, both for the main method described in this paper and for the variant based on (2.19). The results are shown in figure 3. The highest decay lengths occurring in these approximations were $\lambda = 80.1109$ and $\lambda = 13.0905$, respectively. We see that the regions in which serious discrepancies occur differ by an order of magnitude.

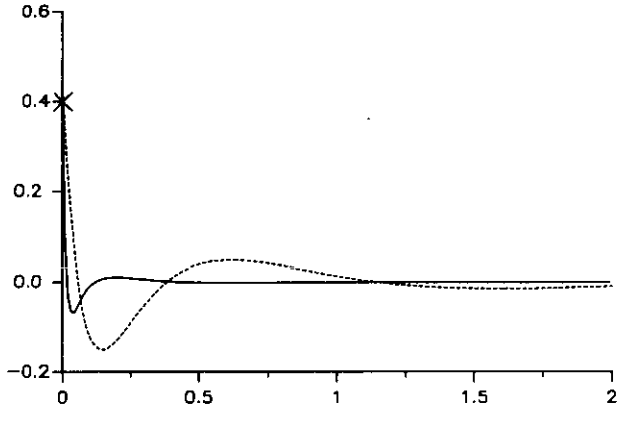

Figure 3. The jump $\Delta_{\mathrm{M}}^{(28)}(x)$ at $v = 0$, defined in (4.8), as a function of x for the Milne solution in the BGK case. In the exact solution, the quantity vanishes for all $x \neq 0$. The exact $x = 0$ value is denoted by a cross.

5. The Milne problem with partial specular reflection

When a fraction r of the particles reaching the wall are reflected specularly there, the boundary condition (3.13) should be replaced by

$$d_{1r}^{\mathrm{M}} = -1 \qquad f_r^{\mathrm{M}}(v, 0) = r f_r^{\mathrm{M}}(-v, 0) \qquad \text{for } v > 0. \tag{5.1}$$

For the Klein-Kramers case the solution around $v = x = 0$ has a particularly sharp singularity [13, 14]

$$f_r^{\mathrm{M}}(-v, 0) = c_0(r) v^{\lambda(r)}[1 + \mathcal{O}(v^2)] \qquad f_r^{\mathrm{M}}(v, 0) = r f_r^{\mathrm{M}}(-v, 0) \qquad \text{for } v > 0 \qquad (5.2a)$$

with $c_0(r)$ a function known only numerically and

$$\lambda(r) = \frac{1}{2} - \frac{3}{\pi} \sin^{-1}\left(\frac{r}{2}\right) \qquad (5.2b)$$

which for $r \to 1$ approaches zero. The degree to which such a sharp singularity is reproduced provides a sensitive test for any method of approximation. Substituting (5.1) into (3.11), using the symmetry of the $\phi_n(v)$, and requiring the coefficients of all $\phi_{n+}(v)$ in this relation to vanish leads to the set of relations

$$\delta_{n0} d_0^{(N)}(1-r) + \sum_{k=1}^{N-1} d_{2k}^{(N)}[b_{n(2k)}^{+(N)} - r(-1)^n b_{n(2k)}^{-(N)}] = \delta_{n1}(1+r) \qquad \text{for } 0 \leqslant n < N \qquad (5.3)$$

from which the N coefficients $d_{2i}^{(N)}$, $0 \leqslant i < N$, can be determined. The resulting $f_r^{\mathrm{M}}(v, 0)$ for the Klein-Kramers case in $N = 25$ approximation are shown in figure 4 for $r = 0.8$, together with the exact asymptotic expansion [14], which includes a few correction terms in addition to the leading term given in (5.2a). Since the results for large v do not differ appreciably from those presented in figure 5(b) of [14], we present here an enlarged view of the neighbourhood of $v = 0$, with some results obtained by earlier methods given for comparison. Also, since the choice of '$\delta(0)$' is expected to be critical for this very singular distribution function, we present results with two different choices for '$\delta(0)$'. We shall comment on these results after table 4.

For the BGK case the Milne problem with partial specular reflection can be reduced to a singular integral equation [15], for which no explicit solution is yet known to us.

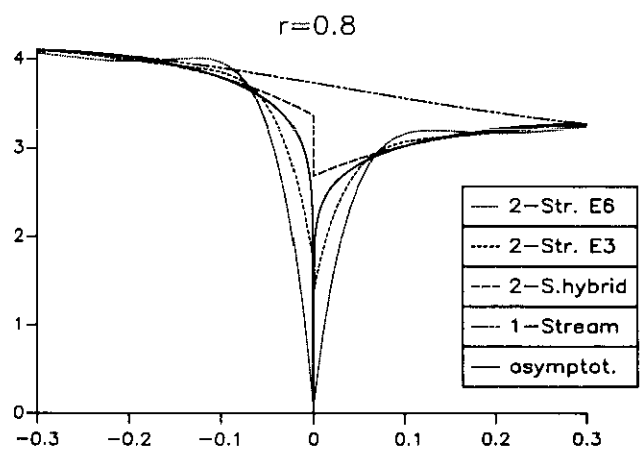

Figure 4. The velocity distribution at the wall for the Milne problem with partial specular reflection in the Klein-Kramers case, with reflection coefficient $r = 0.8$, as obtained in the $N = 50$ one-stream approximation, as well as in $N = 25$ approximation, both with the hybrid (2.19) formalism and with the full two-stream method with values 10^3 and 10^6 for '$\delta(0)$'. The asymptotic approximation to the exact solution for small v is also given. The figure shows only the behaviour close to the singularity at $v = 0$; the behaviour for larger $|v|$ is as in figure 5(b) of [14].

Asymptotically for small positive v one obtains

$$f_r^{\mathrm{M}}(-v,0)=\frac{n^r(0)}{\sqrt{2\pi}}\left[1-\frac{1-r}{\sqrt{2\pi}}v\ln v\right]+\mathcal{O}(v)$$
$$f_r^{\mathrm{M}}(v,0)=rf_r^{\mathrm{M}}(-v,0) \tag{5.4}$$

with $n^r(0)$ the density at the wall, which can only be determined from the full solution. In figure 5 we show the $N=25$ approximation to the BGK solution for $r=0.5$, together with the exact expression, as evaluated using the techniques described in [15], and the one-stream result.

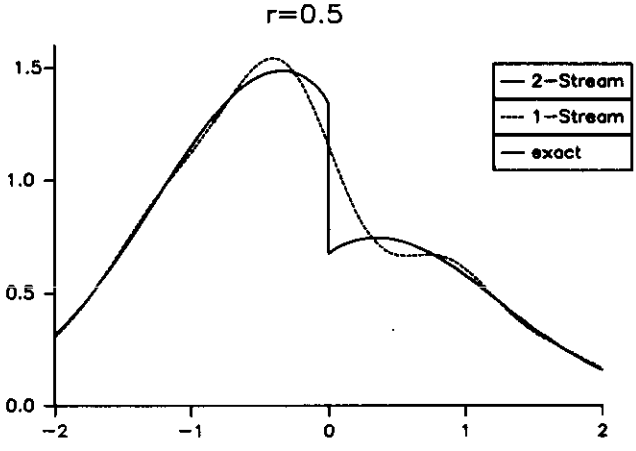

Figure 5. The velocity distribution at the wall for the Milne problem with partial specular reflection in the BGK case for reflection coefficient $r=0.5$, as obtained from the one-stream $N=50$ and the two-stream $N=25$ approximation, as well as from the exact solution (exact and two-stream results are indistinguishable).

The extrapolation procedure (4.2) can again be used to obtain accurate values for some characteristic quantities. The Milne length $x_{\mathrm{M}}^r \equiv d_{0r}^{\mathrm{M}}$ can thus be determined up to 8 significant figures in the Klein-Kramers case and up to 10 significant figures in the BGK case. As a numerical test for the quality of the distribution functions we calculated the quantity

$$\tilde{\Delta}_{\mathrm{M}r}=\sqrt{\frac{2}{\pi}}\frac{1-r}{1+r}\Delta_{\mathrm{M}r} \tag{5.5}$$

with $\Delta_{\mathrm{M}r}$ the limiting value of $f_r^{\mathrm{M}}(-v,0)$ for $v\downarrow 0$, which vanishes in the exact solution for the Klein-Kramers case. The prefactor, which becomes equal to $[n_{\mathrm{M}r}(0)]^{-1}$ for $r\to 1$ [14], corrects for the fact that the density at the wall itself depends strongly on r; thus $\tilde{\Delta}_{\mathrm{M}r}$ is a better measure of the quality of the distribution than $\Delta_{\mathrm{M}r}$ itself. The results for several r in the Klein-Kramers case are given in table 4. The results obtained using the hybrid representation (2.19) are given for comparison.

From the results in figure 4 and table 4 one sees that the actual distribution function is approached in a qualitatively different way in the two versions of the two-stream method. In the hybrid method, the deep minimum at $v=0$ is not reproduced very well; on the other hand, the two limiting values for $v\to\pm 0$ depend regularly on N and the (4.2) fits indicate an approach to zero. For the more consistent two-stream method the

Table 4. The scaled value $\tilde{\Delta}_{M,r}$, defined in (5.5), for the Milne problem with partial specular reflection in the Klein-Kramers case for different values of the reflection coefficient r, in $N = n$ approximation $(2, n)$. The results obtained from the hybrid formalism based on (2.19) are given as (h, n); those obtained from an extrapolation using (4.2) are indicated by (h, ∞). The tabulated quantity vanishes for the exact solution. Further conventions are as in table 2.

r	$(2, 2)$	$(2, 30)$	$(h, 30)$	(h, ∞)
0.0	0.0156	0.0137	0.0827	0.0067
0.2	0.0193	0.0235	0.1154	0.0114
0.4	0.0254	0.0417	0.1585	0.0185
0.6	0.0369	0.0782	0.2159	0.0324
0.8	0.0675	0.1611	0.2932	0.0799
0.99	0.3203	0.3784	0.3928	—

limiting values for small N are much better than for the hybrid method; with increasing N, however, the results at $v = 0$ actually become slightly worse (except for very small r), and a fit of type (4.2) is not possible. On the other hand, the behaviour for small but finite $|v|$ improves markedly with increasing N. The use of a high value for '$\delta(0)$' leads to a lower minimum, as expected, but the results for finite v become worse and exhibit an 'overshoot'.

6. Some albedo problems

In the albedo problem one studies the boundary layer that develops when particles are injected into the gas at the wall with a given velocity distribution $g(v)$, in the absence of any current coming in from infinity. Such boundary layers may occur near walls that either spontaneously emit particles, as in the case of sublimation or evaporation of an adsorbed liquid layer, or reflect them inelastically, for example with a temperature different from that prevailing in the bulk of the gas. Under the aspect of the approximation scheme presented in this paper it is of interest to study how well the method works even for input functions that are not represented very well by finite sums of half-range Hermite polynomials. For this purpose it suffices to study the class of input distributions

$$g(v) = v^{\alpha} \exp[-\beta v^2/2][j^+(\alpha, \beta)]^{-1} \tag{6.1a}$$

where the factor $(j^+)^{-1}$, given by

$$j^+(\alpha, \beta) = \Gamma[1 + (\alpha/2)]\beta^{-1}(\beta/2)^{-\alpha/2} \tag{6.1b}$$

ensures that the total injected current is unity. This class of functions includes, for $\alpha = 0$, the important case of thermal injection; moreover the singularity structure for this case was studied recently [14, 15].

For the expansion coefficients g_n defined in (3.16) we obtain, separately for even and odd n:

$$g_{2n}(\alpha, \beta) = \frac{(-1)^n(2n-1)!!}{2\sqrt{(2n)!}} \frac{\Gamma[(\alpha+1)/2]}{\Gamma[(\alpha+2)/2]} \sqrt{2\beta}\, {}_2F_1\left(-n, \frac{\alpha+1}{2}, \frac{1}{2}, \frac{1}{\beta}\right) \tag{6.2a}$$

$$g_{2n+1}(\alpha, \beta) = \frac{(-1)^n(2n+1)!!}{\sqrt{(2n+1)!}} {}_2F_1\left(-n, \frac{\alpha+2}{2}, \frac{3}{2}, \frac{1}{\beta}\right) \tag{6.2b}$$

where ${}_2F_1(a, b, c, x)$ is a hypergeometric function [22]. For $\alpha = 0$ the even coefficients reduce to

$$g_{2n}(0, \beta) = \frac{(2n-1)!!}{2\sqrt{(2n)!}} \sqrt{2\pi\beta} \left(\frac{1}{\beta} - 1\right)^n. \tag{6.3}$$

Some exact results for the albedo problem in the Klein-Kramers case with the form (6.1) for $g(v)$ were given in [14]. For the BGK case, this albedo problem can be solved in closed form [15]. Of particular interest is the quantity d_0, which the $d_0^{(N)}$ in (3.11) should approach for $N \to \infty$; it is equal to the density $n^g(x) = \int dv\, P^g(v, x)$ in the limit $x \to \infty$. For this quantity one obtains [15]

$$d_0^g(\alpha, \beta) = \frac{1}{j^+(\alpha, \beta)} \int_0^\infty dv\, v^{\alpha+1} \exp[-\tfrac{1}{2}\beta v^2 + Q(v)]. \tag{6.4}$$

For the function $Q(v)$ an integral expression similar to the expression (4.7*a*) for x_M^{BGK} can be given: the factor t in the numerator of the integrand must be replaced by $\ln(t+v)$.

To determine the coefficients $d_{2n}^{g(N)}$, as defined in (3.11) and (3.14), we applied the prescription (3.16). This gives rise to the set of equations

$$g_n = a_{n0} d_0^{g(N)} + \sum_{p=1}^{N-1} d_{2p}^{g(N)} \sum_{m=0}^{N-1} a_{nm} b_{m(2p)}^{+(N)} \tag{6.5}$$

where the overlap integrals a_{mn} are given in (2.10). The relation (6.5) can also be written as

$$g_n = \sum_{m=0}^{N-1} a_{nm} q_m \qquad q_m = \delta_{m0} d_0^{g(N)} + \sum_{p=1}^{N-1} d_{2p}^{g(N)} b_{m(2p)}^{+(N)}. \tag{6.6}$$

Since the $N \times N$ truncated version of the infinite matrix a_{nm} has a smallest eigenvalue of order 10^{-N}, we performed a few preliminary tests. For this purpose we took

$$g(v) = \psi_{k+}(v) \qquad g_n = a_{nk}. \tag{6.7}$$

For $N \leqslant k$, (6.6) has the obvious solution $q_m = \delta_{mk}$, whereas for $N \geqslant k$ all q_m become non-zero. Nevertheless, the approximants $d_0^{g(N)}$ depend smoothly on N through $N = k$, in spite of the fact that for N approaching k the q_m derived from (6.5) begin to deviate significantly from the values δ_{mk}. On the other hand, inserting the values $q_m = \delta_{mk}$ into (6.6) did not lead to results significantly different from those obtained by direct use of (6.5).

As a second test we considered the cases $\alpha = 0, \beta = 1$ and $\alpha = 1, \beta = 1$ in (6.1). For the first case, the solution must be a multiple of the equilibrium solution

$$f^g(v, x; 0, 1) = \sqrt{2\pi}\, \psi_0(v) \qquad d_0^g(0, 1) = \sqrt{2\pi}. \tag{6.8}$$

For the second case one concludes from (3.11)–(3.15)

$$f^g(v, x; 1, 1) = 2[f^M(v, x) - x\phi_0(v) + \phi_1(v)] \tag{6.9*a*}$$

$$d_0^g(1, 1) = 2x_M. \tag{6.9*b*}$$

These results were indeed recovered; the accuracy obtained for x_M by this detour was comparable to that of the more direct method presented in section 4.

In figures 6 and 7 we present the results obtained for the velocity distribution at the wall $f^g(v, 0; 0, \beta)$, corresponding to thermal injection at some inverse temperatures β (measured in units of the temperature far from the wall, which is unity in our system

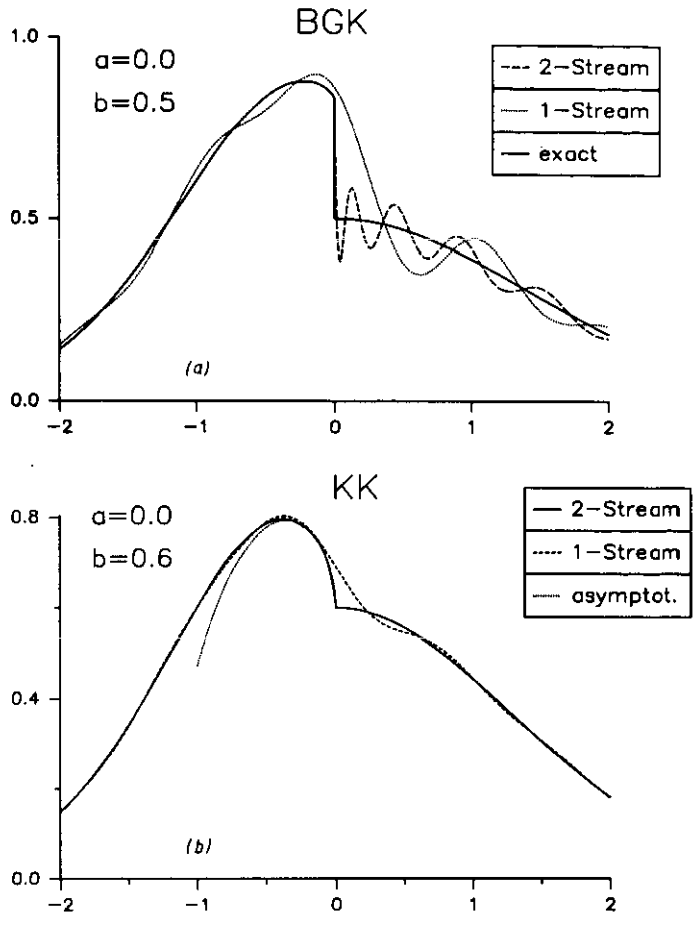

Figure 6. (*a*) The velocity at the wall for the albedo problem with thermal injection at twice the background temperature ($\alpha = 0$, $\beta = 0.5$ in (6.1)) for the BGK case; we show the one-stream $N = 50$, the two-stream $N = 25$ approximation and the exact result. (*b*) The same quantities as in (*a*) for the Klein-Kramers case for $\alpha = 0$, $\beta = 0.6$; for negative v, the exact asymptotic small-v expansion is shown instead of the exact result.

of units) in both the BGK and the Klein-Kramers cases in the $N = 25$ approximation. At the input side ($v > 0$) the exact $g(v)$ is also given for comparison. For the Klein-Kramers case $g(v)$ is known to be continuous at $v = 0$; for the BGK case the jump at $v = 0$ is known [15].

As expected from (6.3), the representation of $g(v)$ (equal to f^g for $v > 0$) becomes poor for $\beta \leqslant 0.5$; this is shown in figure 6(*a*), where one sees that f^g for $v < 0$ is nevertheless reproduced remarkably well for the BGK case. For the Klein-Kramers case f^g is given rather poorly for $\beta = 0.5$ even for negative v (though somewhat better than for $v > 0$), and we present the results for $\beta = 0.6$ instead. The spectacular improvement with respect to the one-stream method is also manifest from the figures. For the more benign case $\beta = 2$, for which the results are given in figure 7, we do not present the one-stream results; instead we combine the BGK and Klein-Kramers results in a single figure, to bring out more clearly the marked difference in the velocity distributions for the returning particles, in spite of the quite similar values for global quantities like

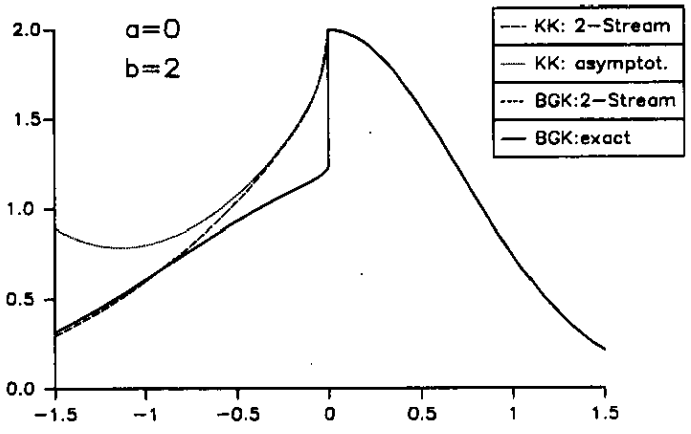

Figure 7. The velocity distributions at the wall for the albedo problem (6.1) with $\alpha = 0$, $\beta = 2$ for the BGK and Klein-Kramers cases; we show the two-stream $N = 25$ approximations as well as the exact asymptotic small-v expansion for the Klein-Kramers case; the exact solution for the BGK case is indistinguishable from the two-stream approximation on the scale of the figure.

$n^g(0)$ and $n^g(\infty)$. To test how well our method functions for non-analytic input distributions $g(v)$ we present the solution $f^g(v, 0; \frac{1}{2}, 1)$ for the Klein-Kramers and BGK cases in figure 8. Again, the distribution of returning particles is indistinguishable from the exact BGK result, at least in the figure.

To assess the ultimate numerical precision attainable with our method (without going beyond extended precision arithmetic) we present in table 5 for the BGK case the results obtained for the global quantities $n^g(\infty)$ and $n^g(0)$, as well as for the limiting value $f^g(0-\varepsilon, 0; \alpha, \beta)$ for several values of α and β. Note that we obtain reasonable results for the global quantities even at $\alpha = 0$, $\beta = 0.35$, where (6.3) indicates a strong divergence of the moment expansion for the input distribution. For still lower β, even our method fails, however. The difference in accuracy obtainable for global and local quantities becomes especially clear for the BGK case, where two of the listed quantities

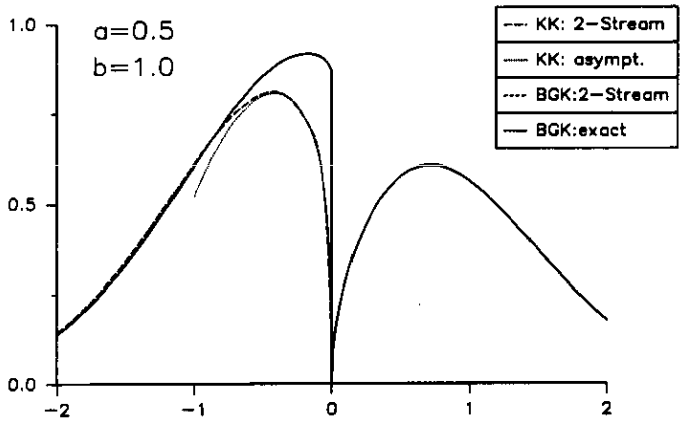

Figure 8. The same quantities as in figure 7 for the singular input distribution (6.1) with $\alpha = 0.5$, $\beta = 1$.

Table 5. The densities at the wall, $n^g(0)$, and at infinity, $n^g(\infty)$, as well as the limit $f^g(0-\varepsilon, 0)$ of the velocity distribution at the wall, for the albedo problem in the BGK case with input distribution $g(v) \sim v^\alpha \exp[-\beta v^2/2]$ for several values of α and β, as obtained in the $N=25$ approximation, $(2N)$, by an extrapolation fit, (2∞), and from the exact analytic solution (ex). Further conventions are as in table 2.

α	β		$n^g(\infty)$	$n^g(0)$	$f^g(-\varepsilon, 0)$
0	0.35	$(2N)$	3.415 030 41	1.892 9057	0.252 427
		(2∞)	3.413	1.92	0.8
		(ex)	3.413 423 80	1.921 1956	0.766 446
0	0.40	$(2N)$	3.271 551 57	1.979 8654	0.776 160
		(2∞)	3.271 5	1.981	0.79
		(ex)	3.271 501 00	1.980 7539	0.790 206
0	0.50	$(2N)$	3.053 621 16	2.088 9274	0.835 198
		(2∞)	3.053 621	2.088 93	0.83
		(ex)	3.053 620 99	2.088 9285	0.833 361
0	1	$(2N)$	$\sqrt{2\pi}+4\times10^{-14}$	$\sqrt{2\pi}+2\times10^{-12}$	$1-10^{-10}$
		(2∞)	$\sqrt{2\pi}+10^{-15}$	$\sqrt{2\pi}+10^{-12}$	—
		(ex)	$\sqrt{2\pi}$	$\sqrt{2\pi}$	1
0	2	$(2N)$	2.110 975 36	3.084 488 3	1.226 222
		(2∞)	2.110 975 601	3.084 488 51	1.230 5
		(ex)	2.110 975 60	3.084 488 5	1.230 532
0	5	$(2N)$	1.747 918 68	4.204 725 9	1.658 780
		(2∞)	1.747 919 7	4.204 726	1.678
		(ex)	1.747 919 69	4.204 7269	1.677 443
0.5	1	$(2N)$	2.701 557 88	2.178 975 6	0.873 473
		(2∞)	2.701 557 610	2.178 977 11	0.869 3
		(ex)	2.701 557 60	2.178 977 4	0.869 286
1	1	$(2N)$	2.874 223 61	$2+3\times10^{-16}$	0.802 267
		(2∞)	2.874 223 3715	—	0.797 88
		(ex)	2.874 223 37	2	0.797 884

are linked by the relation

$$f^g(0-\varepsilon, x) = n^g(x)/\sqrt{2\pi} \tag{6.10}$$

which follows from the structure of the BGK collision operator [15]. We do not present comparable data for the Klein-Kramers case, since there the exact result cannot be evaluated to the precision required, except for $\beta = 1$, $\alpha = 0$ or 1, where a closed form solution is available as discussed earlier in connection with (6.8)-(6.9). For the latter cases accuracies comparable to the BGK case are obtained.

7. Concluding remarks

The results obtained in this paper fully confirm the conjecture by Gross *et al* [16] and by Razi Naqvi *et al* [17] that an expansion in half-range functions of the velocity yields better numerical results for boundary value problems than expansions in full-range functions, which at first sight appear safer mathematically. Moreover, a persistent

use of half-range representations throughout the formalism yields results superior to those of the less adventurous mixed formalism based on (2.19), which is closer in spirit to the treatment in [17]. As is clear from the comparison with exact results, neither the use of a basis that becomes overcomplete in the limit $N \to \infty$, nor the occurrence of formally infinite matrix elements in the Klein-Kramers case has adverse effects, though they compel us to use extended precision arithmetic.

The method developed in this paper is in no way restricted to the two special collision operators considered; it can be applied to any linear semidefinite operator $\mathscr{C}$. Also, as mentioned before, it can be applied to the Laplace transform of a time-dependent linear kinetic equation. When the eigenvalue zero is degenerate, the number of Chapman-Enskog solutions also increases, as extensively discussed elsewhere [23, 24]. In actual physical systems, it does not usually suffice to consider only one velocity variable, even when considering a half-space $x>0$ and situations in which the boundary conditions, and hence the solution, do not depend on the variables y and z. For the two collision operators considered, all eigenfunctions of $\mathscr{C}$ can be written in the form [12]

$$\phi_{nl}(\boldsymbol{v}) = \text{constant} \times \phi_0(v) H_n\left(\frac{v_x}{\sqrt{2}}\right) L_l(\tfrac{1}{2}v_t^2) \qquad v_t^2 = v_y^2 + v_z^2 \tag{7.1}$$

where $L_l(\xi)$ is the lth Laguerre polynomial. We may then expand the solution and the boundary conditions in terms of the L_l and then obtain separate boundary value problems for each l, which can be treated with the methods developed in this paper. For more general collision operators, an expansion in terms of the half-space Burnett functions

$$\psi_{nk\sigma}(v, \mu) = \psi_{nk}(v, \mu)\Theta(\sigma\mu) \qquad \mu = \hat{v} \cdot \hat{r} \tag{7.2}$$

with ψ_{nk} the ordinary Burnett functions [25], may be more convenient, since collision operators derived from centrally symmetric interactions do not couple ψ_{nk} with different k. We tested our scheme for expansions in the functions (7.2) as well, and obtained identical results for the sequence of truncations S_N, in which the coefficients of all $\psi_{nk\sigma}$ with $2n+k \geqslant N$ are put equal to zero. Truncations with $n+k<N$ [24] give results of slightly lesser quality.

A generalization to problems with spherical or cylindrical symmetry is considerably less straightforward, since the *radial* velocity, unlike the component of the velocity perpendicular to a plane wall, is not a constant of the motion during the free flow. For not too small R, however, an expansion of the solution in powers of R^{-1} [26] reduces the spherically symmetric problem to a sequence of planar problems, with the solution of the problem in order k serving as input function for an albedo problem in order $k+1$. In view of the high accuracy obtainable with the present method, it may be possible to obtain reliable results for several orders in R^{-1}, and hence to study the convergence of the expansion and to estimate the range of R-values for which it can yield reliable results.

Acknowledgment

This work was supported by the Fonds zur Förderung der Wissenschaftlichen Forschung in Österreich.

References

[1] Klein O 1922 *Ark. Mat. Astron. Fys.* **16**(5) 1
[2] Kramers H A 1940 *Physica* **7** 284
[3] Bhatnagar P L, Gross E P and Krook M 1954 *Phys. Rev.* **94** 511
Welander P 1954 *Ark. Fys.* **7** 507
[4] Cercignani C 1988 *The Boltzmann Equation and its Applications* (Berlin: Springer)
[5] Case K M 1960 *Ann. Phys., NY* **9** 1
Cercignani C 1962 *Ann. Phys., NY* **20** 219; 1964 *Ann. Phys., NY* **40** 469
[6] Marshall T W and Watson E J 1985 *J. Phys. A: Math. Gen.* **18** 3531; 1987 *J. Phys. A: Math. Gen.* **20** 1345
[7] Pagani C D 1970 *Boll. Un. Mat. Ital.* **3** 961
[8] van Kampen N G 1955 *Physica* **21** 949; Case [5]
[9] Burschka M A and Titulaer U M 1981 *J. Stat. Phys.* **25** 569
[10] Titulaer U M 1984 *J. Stat. Phys.* **37** 589
[11] Waldenstrøm S, Razi Naqvi K and Mork K J 1983 *Phys. Rev.* A **28** 1659 and references quoted therein
[12] Widder M E and Titulaer U M 1989 *J. Stat. Phys.* **56** 471
[13] Titulaer U M 1985 *Phys. Lett.* **108A** 19
[14] Kainz A J and Titulaer U M 1991 *J. Phys. A: Math. Gen.* **24** 4677
[15] Kainz A J and Titulaer U M to be published
[16] Gross E P, Jackson E A and Ziering S 1957 *Ann. Phys., NY* **1** 141
Gross E P and Ziering S 1958 *Phys. Fluids* **1** 215; 1959 *Phys. Fluids* **2** 701
[17] Razi Naqvi K, Mork K J and Waldenstrøm S 1989 *Phys. Rev.* A **40** 3405
[18] Harris S 1981 *J. Chem. Phys.* **75** 3103
[19] Titulaer U M 1978 *Physica* **91A** 321; 1980 *Physica* **100A** 234
[20] Beals R and Protopopescu V 1983 *J. Stat. Phys.* **32** 565
[21] Marshak R E 1947 *Phys. Rev.* **71** 443
[22] Olver F W J 1974 *Asymptotics and Special Functions* (New York: Academic)
[23] Vestner H and Waldmann L 1977 *Z. Naturforsch.* A **32** 667
Waldmann L and Vestner H 1979 *Physica* **99A** 1
[24] Hubmer G F and Titulaer U M 1990 *J. Stat. Phys.* **59** 441; 1991 *J. Stat. Phys.* **63** 203
[25] Ferziger J H and Kaper H G 1972 *Mathematical Theory of Transport Processes in Gases* (Amsterdam: North-Holland)
[26] Widder M E and Titulaer U M 1989 *J. Stat. Phys.* **55** 1109